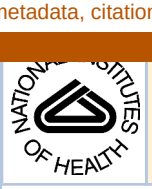

Published in final edited form as:

Ann N Y Acad Sci. 2009 March ; 1157: 61–70. doi:10.1111/j.1749-6632.2008.04119.x.

Simultaneous Electroencephalography and Functional Magnetic Resonance Imaging of General Anesthesia

Patrick L. Purdon[1,2,6], **Eric T. Pierce**[1], **Giorgio Bonmassar**[3,2], **John Walsh**[1], **P. Grace Harrell**[1], **Jean Kwo**[1], **Daniel Deschler**[8], **Margaret Barlow**[4], **Rebecca C. Merhar**[1], **Camilo Lamus**[6], **Catherine M. Mullaly**[1], **Mary Sullivan**[5], **Sharon Maginnis**[5], **Debra Skoniecki**[5], **Helen-Anne Higgins**[5], and **Emery N. Brown**[1,6,7]

[1] Department of Anesthesia and Critical Care, Massachusetts General Hospital, Boston, MA

[2] Athinoula A. Martinos Center for Biomedical Imaging, Massachusetts General Hospital, Charlestown, MA

[3] Department of Radiology, Massachusetts General Hospital, Boston, MA

[4] Department of Neurology, Massachusetts General Hospital, Boston, MA

[5] Clinical Research Center, Massachusetts General Hospital, Boston, MA

[6] Department of Brain and Cognitive Sciences, Massachusetts Institute of Technology, Cambridge, MA

[7] Division of Health Sciences and Technology, Massachusetts Institute of Technology, Cambridge, MA

[8] Massachusetts Eye and Ear Infirmary, Boston, MA

Abstract

It has been long appreciated that anesthetic drugs induce stereotyped changes in electroencephalogram (EEG), but the relationships between EEG and underlying brain function remain poorly understood. Functional imaging methods including positron emission tomography (PET) and functional magnetic resonance imaging (fMRI), have become important tools for studying how anesthetic drugs act in the human brain to induce the state of general anesthesia. To date, no investigation has combined functional MRI with EEG to study general anesthesia. We report here a paradigm for conducting combined fMRI and EEG studies of human subjects under general anesthesia. We discuss the several technical and safety problems that must be solved to undertake this type of multimodal functional imaging and show combined recordings from a human subject. Combined fMRI and EEG exploits simultaneously the high spatial resolution of fMRI and the high temporal resolution of EEG. In addition, combined fMRI and EEG offers a direct way to relate established EEG patterns induced by general anesthesia to changes neural activity in specific brain regions as measured by changes in fMRI blood oxygen level dependent (BOLD) signals.

1. Introduction

General anesthesia is a drug-induced, reversible condition comprised of five behavioral states: hypnosis (loss of consciousness), amnesia (loss of memory), analgesia (loss of pain sensation), akinesia (immobility), and hemodynamic stability with control of the stress response [1]. Use of

Address for correspondence: Patrick L. Purdon, Department of Anesthesia and Critical Care, Massachusetts General Hospital, 55 Fruit Street, Gray Bigelow 444 Boston, MA 02114.patrickp@nmr.mgh.harvard.edu.

general anesthesia in the United States began in the 1840's and literally overnight, transformed surgery here and in Europe from butchery to a humane therapy 2. It is estimated that over 100,000 patients receive general anesthesia each day in the United States for surgical procedures alone 3. General anesthesia and conscious sedation are also widely used for non-surgical interventions in critical care, radiology, obstetrics, pediatrics, gastroenterology, and dentistry. Since World War II there have been significant improvements in anesthetic drugs, and in anesthetic delivery, and monitoring systems. Nevertheless, the mechanisms by which anesthetic drugs create and sustain the state of general anesthesia remain one of the biggest mysteries of modern medicine 4.

Current approaches to studying the mechanisms of action of general anesthetics focus primarily on characterizing the binding properties of anesthetic drugs to receptor sites in the brain and spinal cord [5–9]. This important work has helped identify common molecular and pharmacological principles that underlie anesthetic drugs. They have also been important for establishing that there are several rather than a single mechanism of anesthetic action. Another focus of anesthesia drug research has been the study of the pharmacokinetic and pharmacodynamic properties of drugs [10, 11]. This research provides the main guidelines for anesthetic drug dosing.

Although functional imaging studies of general anesthesia are also becoming more prevalent [12–24], they are not as prevalent as functional imaging studies of other neuroscience questions. To date, no studies of general anesthesia have combined different imaging modalities such as functional magnetic resonance imaging (fMRI) and the electroencephalogram (EEG). Combining fMRI and EEG would make it possible to exploit simultaneously the high spatial resolution of fMRI and the high temporal resolution of EEG [25, 26] in human studies of mechanisms of general anesthesia. Furthermore, combining fMRI with EEG offers the potential to relate the large body of information in the anesthesiology literature on EEG pattern changes under general anesthesia to changes in neural activity in specific brain sites.

To develop this multimodalimaging paradigm, several technical and safety problems must be solved. First, because magnetic resonance imaging employs powerful static magnetic, gradient magnetic, and radiofrequency fields, the EEG acquisition system and electrodes must be designed and constructed to minimize physical interactions with these fields that can result in subject injury or compromise data quality [26, 27]. Second, the same standards of physiological monitoring for general anesthesia administered in the operating room, which includes, blood pressure, heart rate, oxygen saturation, oxygen delivery, end tidal carbon dioxide must be maintained during these studies [28]. Third, all of the anesthesia equipment, including the anesthesia machine, must be MRI compatible. Finally, because apnea is an expected response following administration of potent hypnotic anesthetic drugs, airway management and ventilation must be carried out while the subject is being imaged under general anesthesia with the same standards of care as in the operating room. We here report a paradigm to conduct combined fMRI and EEG studies of human subjects under general anesthesia.

2. Methods

Subjects

Eight volunteer subjects, 50–60 years old, with preexisting tracheal stomas but with no other significant medical conditions (American Society of Anesthesiologists (ASA) Physical Status II) gave written consent to participate in this study approved by the Massachusetts General Hospital (MGH) Department of Anesthesia and Critical Clinical Practices Committee, the MGH Human Research Committee and the MGH General Clinical Research Center. Potential subjects were first evaluated based on responses to a screening questionnaire to eliminate any subjects with active or chronic, unstable health problems, implying an ASA score greater than

II, and subjects with any contraindications to receiving an fMRI scan. Each subject who passed this initial screening then had a detailed review of his/her medical history, and received a physical examination. Additional tests included an electrocardiogram, a chest X-ray, a urine drug test and for female subjects, a pregnancy test. Any subject whose medical evaluation did not allow him or her to be classified as an ASA II was excluded from the study. Other exclusion criteria included neurological abnormalities and use of either prescribed or recreational psychoactive drugs.

Subject Preparation, Monitoring, and Safety

Subjects were instructed to take nothing by mouth after midnight of the day prior to the study. The urine drug test and pregnancy test, for female subjects, were repeated on the morning of the study. An 18 gauge intravenous catheter was in an antecubital vein for infusion of maintenance fluids and subsequent drug delivery. A 20 gauge radial arterial catheter was placed for continuous blood pressure monitoring. Catheter insertions were preceded by subcutaneous injection of 1% lidocaine. Following topical anesthesia with 4% lidocaine spray, a cuffed 6 or 7 millimeter internal diameter tracheostomy tube (SIMS Portex, Keene, NH) was inserted and secured in place. The tracheostomy tube was later connected to an MRI-compatible anesthesia machine (Ohmeda Excel 210MRI; GE Healthcare, Milwaukee, WI) for oxygenation and ventilation prior to positioning subject in fMRI scanner. Capnography, pulse oximetry, electrocardiogram, and arterial blood pressure were recorded continuously using an MRI-compatible physiological monitor (InVivo Magnitude; InVivo Corporation, Orlando, FL). Subjects were allowed to breathe spontaneously 30% oxygen. Ventilation was assisted manually during propofol administration as needed to maintain end-tidal carbon dioxide ($EtCO_2$) concentration and partial pressure of carbon dioxide CO_2 within 5% of baseline values. Phenylephrine, an alpha-adrenergic agonist [29] that does not affect cerebral blood flow [30], was administered as needed through an intravenous infusion to ensure that mean arterial pressure did not decrease more than 20% from the baseline value.

Several measures were instituted to maximize subject safety during this study. Massachusetts General Hospital Department of Anesthesia and Critical Care standards for off-site administration of anesthesia were followed, including requirements for monitoring (ECG, SpO_2, $ETCO_2$, blood pressure), resuscitation (code cart, ACLS-certified study staff), backup air and oxygen, and backup electrical power, provided by two uninterruptible power supplies (APC SUA-750XL with UXBP24 battery; American Power Conversion Corporation, West Kingston, RI). One anesthesiologist was responsible solely for the medical management of the subject during the study, a second anesthesiologist controlled the propofol infusion and a third anesthesiologist performed the blood sampling. In addition, at least two other medical personnel trained in advanced cardiac life-support, often other anesthesiologists, were also present at each study to assist in the event of an emergency. Prior to the start of each study, an evacuation drill was conducted to ensure that, in the event of an emergency, the subject could be removed from the MRI scanner within approximately 90 seconds. Upon completion of the study the subject was first allowed to recover for a brief period in a monitoring area immediately adjacent to the scanning bay. The subject was then transported to the General Clinical Research Center where the balance of the recovery was completed. The subject was discharged from the recovery area and follow-up was performed in accordance with the standard MGH protocol for discharge following general anesthesia for same-day surgery.

Propofol Administration, Blood Sampling, and Blood Gas Measurement

Propofol was infused intravenously using a previously validated computer-controlled delivery system running STANPUMP[11] connected to a Harvard 22 syringe pump (Harvard Apparatus, Holliston, MA). Five effect-site target concentrations (0.0, 1.0, 2.0, 3.0 and 4.0 mcg/ml) were each maintained for 15 minutes respectively, with a 6.5 minute equilibration period prior to

each propofol level. The 6.5 minutes corresponded to four propofol effect-site equilibration half-lives [31] (Fig. 1, top panel). The infusion was guided by a pharmacokinetic and pharmacodynamic model described in 31, [32] that is part of the STANPUMP program. Plasma samples for propofol concentrations were drawn every five minutes (beginning, middle and end) at each target concentration (Fig. 1, top panel, green arrows). At the end of each target concentration, an additional blood sample was drawn for arterial blood gas analysis (Fig. 1, top panel, blue arrows), performed using an iSTAT Portable Clinical Analyzer with EG3+ blood gas cartridge (Abbot Laboratories, East Windsor, NJ). The propofol infusion was stopped at the end of the last effect-site target period, the subject was removed from the MRI scanner, and allowed to recover.

Auditory Stimulus and Behavioral Task

Auditory stimuli were presented to elicit the 40-Hz auditory steady-state response (ASSR) and auditory blood oxygen level dependent (BOLD) fMRI response, and to devise a clinical measure of loss of consciousness. Subjects were presented 30-second trains of 12.5 millisecond noise bursts repeated at a rate of 40-Hz, in a 30-second stimulus ON, 30-second stimulus OFF pattern over the duration of each propofol level (Fig. 1, bottom panel). Meanwhile, 10 seconds after the end of each 30-second ON period, a 500 millisecond tone was presented (Fig. 1, bottom panel). The tone was randomized between either a low pitch (220 Hz) or high pitch (440 Hz), and the presence or absence of a response within 10 seconds of presentation, the correctness of the response, and the response time, were recorded to define loss of consciousness clinically. Stimuli were delivered using a laptop computer running Presentation (Neurobehavioral Systems, Inc., Albany, CA) with an Echo Indigo 24-bit PCMCIA audio card (Echo Digital Audio Corporation, Carpinteria, CA) and Koss ESP-950 electrostatic headphones retrofitted for MRI-compatibility (Koss Corporation, Milwaukee, WI) or MR Confon Optime 1 headphones (MR Confon, Madeburg, Germany).

Simultaneous EEG and fMRI

The electroencephalogram was recorded continuously at a rate of 950 Hz during fMRI using an MRI-compatible EEG acquisition system 26 using a 19-channel EEG montage with electrodes arranged according to the International 10/20 system. To prevent radio-frequency heating of the EEG leads during MRI 27, the electrode set was constructed from Marktek FiberOhm carbon fiber wires (Marktek Inc., Chesterfield, MI), featuring a distributed resistance of ~7 Ohm/inch [33], bonded with conductive epoxy (Circuit Works CW2400, Chemtronics, Kennesaw, GA) to Ag/Cl electrodes (Gereonics Inc., Solana Beach, CA). Electrodes were held in place using collodion, with impedances less than 5 kOhm.

Functional MRI was acquired using a Siemens Trio 3 Tesla MRI Scanner (Siemens, Erlangen, German). Acquisitions were arranged according to a “sparse sampling” auditory fMRI paradigm during which 1-second volume acquisitions are followed by a 8 to 10 second silent period to minimize the influence of acoustic scanner noise on auditory BOLD fMRI responses [34]. To minimize cardio-pulsatile brainstem motion and maximize brainstem BOLD fMRI signal-to-noise, cardiac gating was used to trigger volume acquisitions 35. Each fMRI volume was acquired in 1 second followed by a 7.5 second delay period, after which cardiac gating was enabled, producing an effective TR of approximately 9 seconds (Fig. 1, bottom panel). The fMRI volume consisted of coronal-oriented slices positioned to cover the brainstem, midbrain, and auditory cortex (4 mm slice thickness, 1 mm skip, 3.1 × 3.1 mm in-plane resolution, 64×64 matrix, TE = 30, 90-degree flip angle) using a quadrature birdcage Bruker Trio head coil (Bruker Corporation, Billerica, MA) for subjects 1 through 4, and a 12-channel TimTrio head coil (Siemens, Erlangen, Germany) for subjects 5 through 8. Prospective acquisition correction (PACE) was used in subjects 5 through 8 for online motion correction during fMRI image acquisition [36]. Structural MRI was acquired using a T1-weighted

MPRAGE sequence (1.3 mm slice thickness, 1.3 × 1 mm in-plane resolution, TR/TE = 2530/3.3 msec, 7-degree flip angle).

Data Analysis

The ASSR was computed in the frequency domain using multi-taper spectral analysis [37] from 4-second EEG windows (M1→Cz) centered 4-seconds prior to each volume acquisition (Fig. 1, bottom panel). For each window, the EEG was linearly detrended and power spectra were computed and averaged across each level for stimulus ON and OFF conditions using the multi-taper method [37], with time-bandwidth product NW = 4. The ratio of the power spectra for stimulus ON versus stimulus OFF was then computed to summarize the 40 Hz ASSR for each level.

Motion correction, registration, and data analysis were performed in AFNI [38], using a general linear model with a 6^{th}-order polynomial for drift correction, and BOLD temporal basis functions previously determined from empirical studies of the auditory BOLD response [39], sampled at the cardiac-gated image acquisition times. Because of the long TR of approximately 9 seconds, T1 correction was not required [40]. Voxel-wise partial F-statistics were computed for the linear combination of BOLD fMRI basis functions, and thresholded at a p-value < 10^{-4} to create activation maps.

3. Results

Across subjects, the average PCO_2 during the study were 37.2±4.5, 37.4±7.3, 38.5±5.8, 39.5 ±6.5, 36.7±7.5 mm Hg for the baseline and target levels 1, 2, 3, and 4, respectively (Table 1 and Figure 2). The PCO_2 levels did not change significantly from baseline, with an average deviation from baseline of −1.43 ± 1.77, 0.13 ± 1.77, 0.98 ± 1.77, and −0.9 ± 2.16 mm Hg for propofol levels 1, 2, 3, and 4, respectively (p = 0.784 from one-way ANOVA, Table 1 and Figure 3).

We illustrate the combined drug infusion, behavioral, EEG, and fMRI paradigm by presenting the results of a single representative subject. The subject lost consciousness during target level 2 (Figure 4). The maximum absolute error in predicted versus assayed plasma propofol concentrations was 0.61 mcg/ml, 0.30, and 0.04 ug/ml at target levels 1, 2, and 3, respectively. The mean error of 0.15±0.25 mcg/ml across all levels (Figure 4, first row). The error was greatest at the 1.0 mcg/ml level, and became progressively smaller at higher concentrations of propofol. For the behavioral task, at baseline level, 15 of 15 (100%) responses were correct, with an average response time of 1.28 ± 0.25 seconds. At level 1, 16 of 21 (76.2 %) responses were correct, 3 were incorrect, and 2 responses were missed, with an average response time of 1.84 ± 0.23 seconds. At level 2, 5 of 21 (24%) responses were correct, 1 was incorrect, and 15 responses were missed, with an average response time of 3.60 ± 0.40. The large number of consecutive missed responses indicated that the study subject had lost consciousness during this level. At level 3, 9 of 9 responses were missed, indicating that loss of consciousness was maintained at this level. Response times for baseline, and levels 1 and 2 were all significantly different from one another ($p < 0.05$ for all pairs of levels under a one-way ANOVA using Scheffe's method for multiple comparisons).

At baseline, a strong ASSR 40 Hz peak was observed in the power spectral ratio (ratio of spectrum at 40 Hz stimulus ON to stimulus OFF), indicating the presence of the 40 Hz ASSR. At level 1, a lower amplitude peak was observed, whereas at levels 2 and 3, no 40 Hz ASSR peak was observed. For the fMRI data, at baseline, activity in response to the 40 Hz stimulus was observed in both primary and secondary auditory cortex. At level 1, activity in secondary auditory cortex was no longer present, but activity in primary auditory cortex was still present. At levels 2 and 3, when the study subject was no longer conscious by our clinical criteria,

primary auditory cortex remained active. In summary, with increasing doses of propofol, we observed progressively fewer correct responses in the auditory tone discrimination task, increasing response times followed by a loss of response, a decrease and then loss of the ASSR, and a decrease in activity in secondary auditory cortex with concomitant maintenance of activity in primary auditory cortex.

4. Discussion

Functional imaging methods have made a tremendous impact in diverse fields such as cognitive neuroscience, psychology, and psychiatry, but have only recently been applied to the problem of general anesthesia. This is in part because of the challenging clinical and physiological confounds associated with general anesthesia, and also due to the inherent difficulty in studying a pharmacological process whose profound effects span the entire central nervous system. Studies using positron emission tomography (PET) to measure anesthesia-induced changes in regional cerebral blood flow (rCBF) [13, 18], or regional glucose metabolism rate (rGMR) [12, 14, 16, 17, 19] revealed dramatic reductions in rCBF and rGMR globally across the entire brain after loss of consciousness, but comparatively smaller interregional differences that made it difficult to identify specific sites of anesthetic action. Functional MRI studies have taken the alternative approach of measuring changes in stimulus-induced activity within specific sensory or cognitive systems during general anesthesia [15, 21–24]. Cerebrovascular confounds pose a serious challenge in fMRI studies of general anesthesia. Inhaled anesthetics are potent cerebral vasodilators, increasing cerebral blood flow (CBF) by 20 to 40% at anesthetic concentrations required to produce unconsciousness [41, 42], potentially saturating the BOLD fMRI response. Meanwhile, general anesthesia-induced apnea can increase PCO_2 and CBF as a consequence, where changes as small as 5 mmHg produce BOLD fMRI signal increases similar in magnitude to those seen during task activity [43].

Our method for multimodal imaging of loss of consciousness under general anesthesia with EEG/fMRI builds upon this prior work. To minimize cerebrovascular confounds, we have chosen to study the drug propofol, which has been shown to preserve cerebral flow metabolism coupling [44–48]. Among inhaled anesthetics, sevoflurane has similar properties [41]. To regulate PCO_2 levels during anesthesia-induced apnea, we studied healthy post-tracheostomy volunteers. By maintaining a secure airway throughout the study using a cuffed tracheostomy tube, we were able to maintain PCO_2 levels within approximately 1.4 mmHg of baseline levels on average, and could image during a gradual progression through general anesthesia-induced states ranging from light sedation to unconsciousness. In order to relate changes in brain activity to anesthesia-induced loss of consciousness, our subjects performed an auditory behavioral task that continually characterized the level of consciousness throughout the protocol. By identifying when the subject stops responding, we are able to clearly identify when the subject is clinically unconscious. Finally, we recorded EEG simultaneously with BOLD fMRI so that clinically-observable EEG and ASSR could be related to site-specific brain activity under general anesthesia.

5. Conclusions

We have established a paradigm for studying general anesthesia using simultaneous EEG and fMRI. In future studies we will use this paradigm to conduct systems level studies of how propofol and other anesthetic drugs alter activity in specific neural circuits to produce the behavioral components of general anesthesia in humans.

Acknowledgments

This work was supported by National Institutes of Health grants DP1-OD003646, K25-NS05758, M01-RR-01066, RR025758-01, R01-EB006385 and the Massachusetts General Hospital Department of Anesthesia and Critical Care.

References

1. Evers, AS.; Crowder, M. Cellular and molecular mechanisms of anesthsia. In: Barash, PG.; Cullen, BF.; Stoelting, RK., editors. Clinical Anesthesia. Lippincott, Williams, & Wilkins; New York: 2006. p. 111-132.
2. Calverley, RK., et al. Anesthesia as a specialty: Past, present, and future. In: Barash, PG.; Cullen, BF.; Stoelting, RK., editors. Clinical Anesthesia. J.B. Lippincott Company; New York: 1989. p. 3-34.
3. Wiklund RA, Rosenbaum SH. Anesthesiology. First of two parts. N Engl J Med 1997;337:1132–1141. [PubMed: 9329935]
4. Kennedy D, Norman C. What don't we know? Science 2005;309:75. [PubMed: 15994521]
5. Franks NP, Lieb WR. Molecular and cellular mechanisms of general anaesthesia. Nature 1994;367:607–614. [PubMed: 7509043]
6. Dilger JP. The effects of general anaesthetics on ligand-gated ion channels. Br J Anaesth 2002;89:41–51. [PubMed: 12173240]
7. Campagna JA, Miller KW, Forman SA. Mechanisms of actions of inhaled anesthetics. N Engl J Med 2003;348:2110–2124. [PubMed: 12761368]
8. Grasshoff C, Rudolph U, Antkowiak B. Molecular and systemic mechanisms of general anaesthesia: the 'multi-site and multiple mechanisms' concept. Curr Opin Anaesthesiol 2005;18:386–91. [PubMed: 16534263]
9. Hemmings HC Jr, et al. Emerging molecular mechanisms of general anesthetic action. Trends Pharmacol Sci 2005;26:503–510. [PubMed: 16126282]
10. Eger EI, Saidman LJ, Brandstater B. Minimum alveolar anesthetic concentration: A standard for anesthetic potency. Anesthesiology 1965;26:756–763. [PubMed: 5844267]
11. Shafer A, et al. Pharmacokinetics and pharmacodynamics of propofol infusions during general anesthesia. Anesthesiology 1988;69:348–356. [PubMed: 3261954]
12. Alkire MT, et al. Cerebral metabolism during propofol anesthesia in humans studied with positron emission tomography. Anesthesiology 1995;82:393–403. [PubMed: 7856898]
13. Veselis RA, et al. Midazolam changes cerebral blood flow in discrete brain regions: an H2(15)O positron emission tomography study. Anesthesiology 1997;87:1106–1117. [PubMed: 9366463]
14. Alkire MT, et al. Positron emission tomography study of regional cerebral metabolism in humans during isoflurane anesthesia. Anesthesiology 1997;86:549–557. [PubMed: 9066320]
15. Antognini JF, et al. Isoflurane anesthesia blunts cerebral responses to noxious and innocuous stimuli: a fMRI study. Life Sci 1997;61:L-54.
16. Alkire MT. Quantitative EEG correlations with brain glucose metabolic rate during anesthesia in volunteers. Anesthesiology 1998;89:323–333. [PubMed: 9710389]
17. Alkire MT, et al. Functional brain imaging during anesthesia in humans: effects of halothane on global and regional cerebral glucose metabolism. Anesthesiology 1999;90:701–709. [PubMed: 10078670]
18. Fiset P, et al. Brain mechanisms of propofol-induced loss of consciousness in humans: a positron emission tomographic study. J Neurosci 1999;19:5506–5513. [PubMed: 10377359]
19. Alkire MT, Haier RJ, Fallon JH. Toward a unified theory of narcosis: brain imaging evidence for a thalamocortical switch as the neurophysiologic basis of anesthetic-induced unconsciousness. Conscious Cogn 2000;9:370–386. [PubMed: 10993665]
20. Bonhomme V, et al. Propofol Anesthesia and Cerebral Blood Flow Changes Elicited by Vibrotactile Stimulation: A Positron Emission Tomography Study. J Neurophysiol 2001;85:1299–1308. [PubMed: 11247998]
21. Heinke W, et al. Sequential effects of propofol on functional brain activation induced by auditory language processing: an event-related functional magnetic resonance imaging study. Br J Anaesth 2004;92:641–650. [PubMed: 15064248]

22. Kerssens C, et al. Attenuated brain response to auditory word stimulation with sevoflurane: a functional magnetic resonance imaging study in humans. Anesthesiology 2005;103:11–19. [PubMed: 15983451]

23. Plourde G, et al. Cortical processing of complex auditory stimuli during alterations of consciousness with the general anesthetic propofol. Anesthesiology 2006;104:448–57. [PubMed: 16508391]

24. Davis MH, et al. Dissociating speech perception and comprehension at reduced levels of awareness. Proc Natl Acad Sci U S A 2007;104:16032–7. [PubMed: 17938125]

25. Bonmassar G, et al. Spatiotemporal brain imaging of visual-evoked activity using interleaved EEG and fMRI recordings. Neuroimage 2001;13:1035–1043. [PubMed: 11352609]

26. Purdon PL, et al. An Open-Source Hardware and Software System for Acquisition and Real-Time Processing of Electrophysiology during High Field MRI. J Neuroscience Methods 2008;175:165–186.

27. Angelone LM, et al. Metallic electrodes and leads in simultaneous EEG-MRI: specific absorption rate (SAR) simulation studies. Bioelectromagnetics 2004;25:285–295. [PubMed: 15114638]

28. Cooper JB, Newbower RS, Kitz RJ. An analysis of major errors and equipment failures in anesthesia management: considerations for prevention and detection. Anesthesiology 1984;60:34–42. [PubMed: 6691595]

29. Goodman, LS., et al. Goodman & Gilman's the pharmacological basis of therapeutics. McGraw-Hill; New York: 2001.

30. Strebel SP, et al. The impact of systemic vasoconstrictors on the cerebral circulation of anesthetized patients. Anesthesiology 1998;89:67–72. [PubMed: 9667295]

31. Schnider TW, et al. The influence of age on propofol pharmacodynamics. Anesthesiology 1999;90:1502–1516. [PubMed: 10360845]

32. Schnider TW, et al. The influence of method of administration and covariates on the pharmacokinetics of propofol in adult volunteers. Anesthesiology 1998;88:1170–1182. [PubMed: 9605675]

33. Angelone, LM.; Bonmassar, G. Use of resistances and resistive leads: Implications on computed electric field and SAR values. Proc. 12th ISMRM1652; 2004.

34. Hall DA, et al. "Sparse" temporal sampling in auditory fMRI. Hum Brain Mapp 1999;7:213–223. [PubMed: 10194620]

35. Harms MP, Melcher JR. Sound repetition rate in the human auditory pathway: representations in the waveshape and amplitude of fMRI activation. J Neurophysiol 2002;88:1433–1450. [PubMed: 12205164]

36. Thesen S, et al. Prospective acquisition correction for head motion with image-based tracking for real-time fMRI. Magn Reson Med 2000;44:457–65. [PubMed: 10975899]

37. Percival, DB.; Walden, AT. Spectral analysis for physical applications. Cambridge University Press; New York: 1993.

38. Cox RW. AFNI: software for analysis and visualization of functional magnetic resonance neuroimages. Comput Biomed Res 1996;29:162–173. [PubMed: 8812068]

39. Harms MP, Melcher JR. Detection and quantification of a wide range of fMRI temporal responses using a physiologically-motivated basis set. Hum Brain Mapp 2003;20:168–183. [PubMed: 14601143]

40. Guimaraes AR, et al. Imaging subcortical auditory activity in humans. Hum Brain Mapp 1998;6:33–41. [PubMed: 9673661]

41. Matta BF, et al. Direct cerebral vasodilatory effects of sevoflurane and isoflurane. Anesthesiology 1999;91:677–680. [PubMed: 10485778]

42. Matta BF, Mayberg TS, Lam AM. Direct cerebrovasodilatory effects of halothane, isoflurane, and desflurane during propofol-induced isoelectric electroencephalogram in humans. Anesthesiology 1995;83:980–985. [PubMed: 7486184]

43. Hoge RD, et al. Investigation of BOLD signal dependence on cerebral blood flow and oxygen consumption: the deoxyhemoglobin dilution model. Magn Reson Med 1999;42:849–863. [PubMed: 10542343]

44. Werner C, et al. The effects of propofol on cerebral and spinal cord blood flow in rats. Anesth Analg 1993;76:971–975. [PubMed: 8484553]

45. Enlund M, et al. Cerebral normoxia in the rhesus monkey during isoflurane- or propofol- induced hypotension and hypocapnia, despite disparate blood-flow patterns. A positron emission tomography study. Acta Anaesthesiol Scand 1997;41:1002–1010. [PubMed: 9311398]

46. Doyle PW, Matta BF. Burst suppression or isoelectric encephalogram for cerebral protection: evidence from metabolic suppression studies. Br J Anaesth 1999;83:580–584. [PubMed: 10673873]

47. Lagerkranser M, Stange K, Sollevi A. Effects of propofol on cerebral blood flow, metabolism, and cerebral autoregulation in the anesthetized pig. J Neurosurg Anesthesiol 1997;9:188–193. [PubMed: 9100192]

48. Newman MF, et al. Cerebral physiologic effects of burst suppression doses of propofol during nonpulsatile cardiopulmonary bypass. CNS Subgroup of McSPI. Anesth Analg 1995;81:452–457. [PubMed: 7653803]

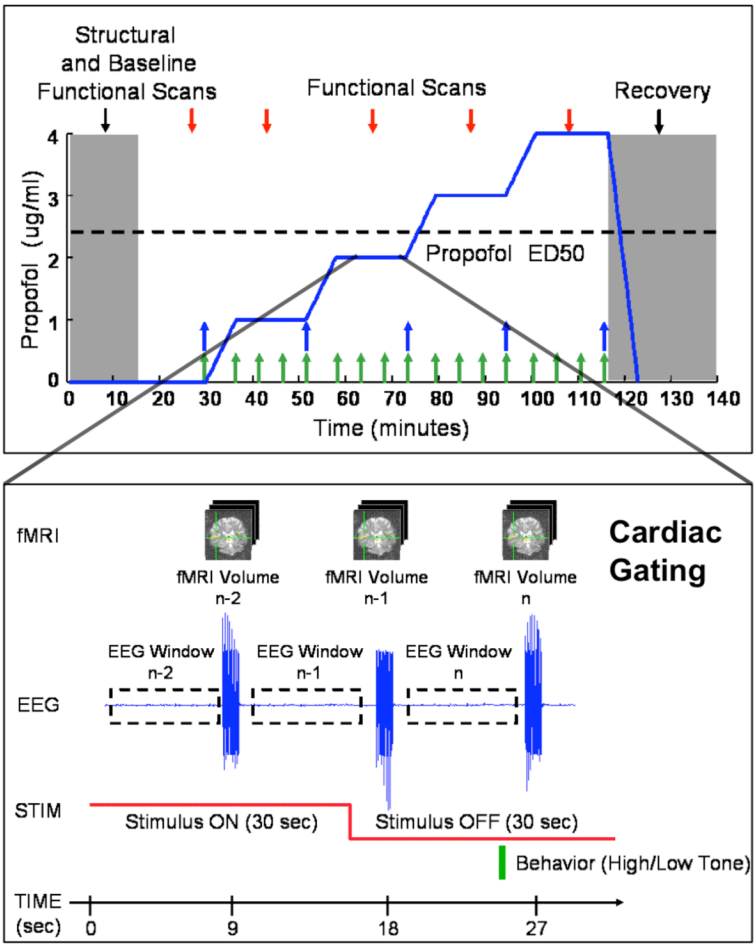

Figure 1.

Study protocol diagram, showing propofol effect-site target concentrations (top), propofol blood sampling (top, green arrows), PCO_2 blood sampling (top, blue arrows), "sparse-sampled" fMRI data acquisition paradigm (bottom), EEG windows (bottom), auditory stimuli with both 40 Hz noise bursts (bottom, red line) and behavioral task (bottom, green bar).

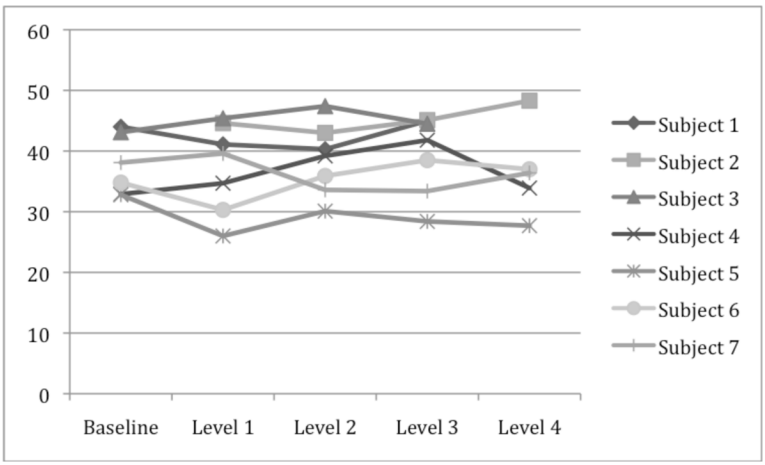

Figure 2.
PCO_2 values measured during study.

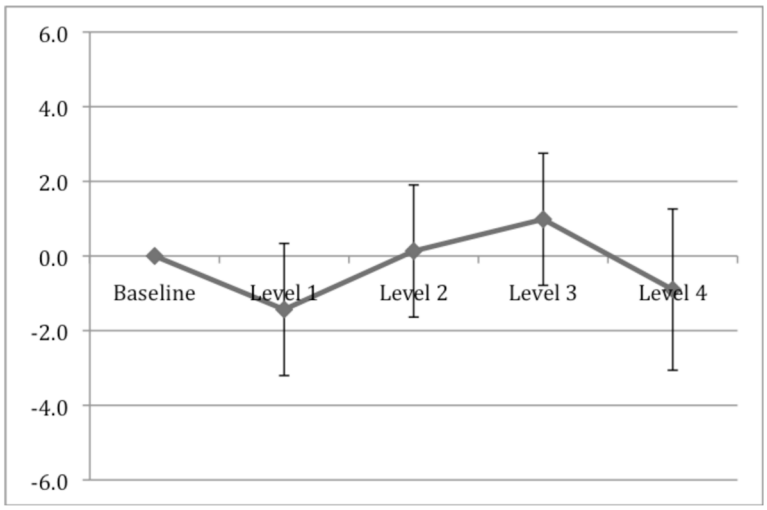

Figure 3.
Deviation of PCO_2 levels from baseline during study.

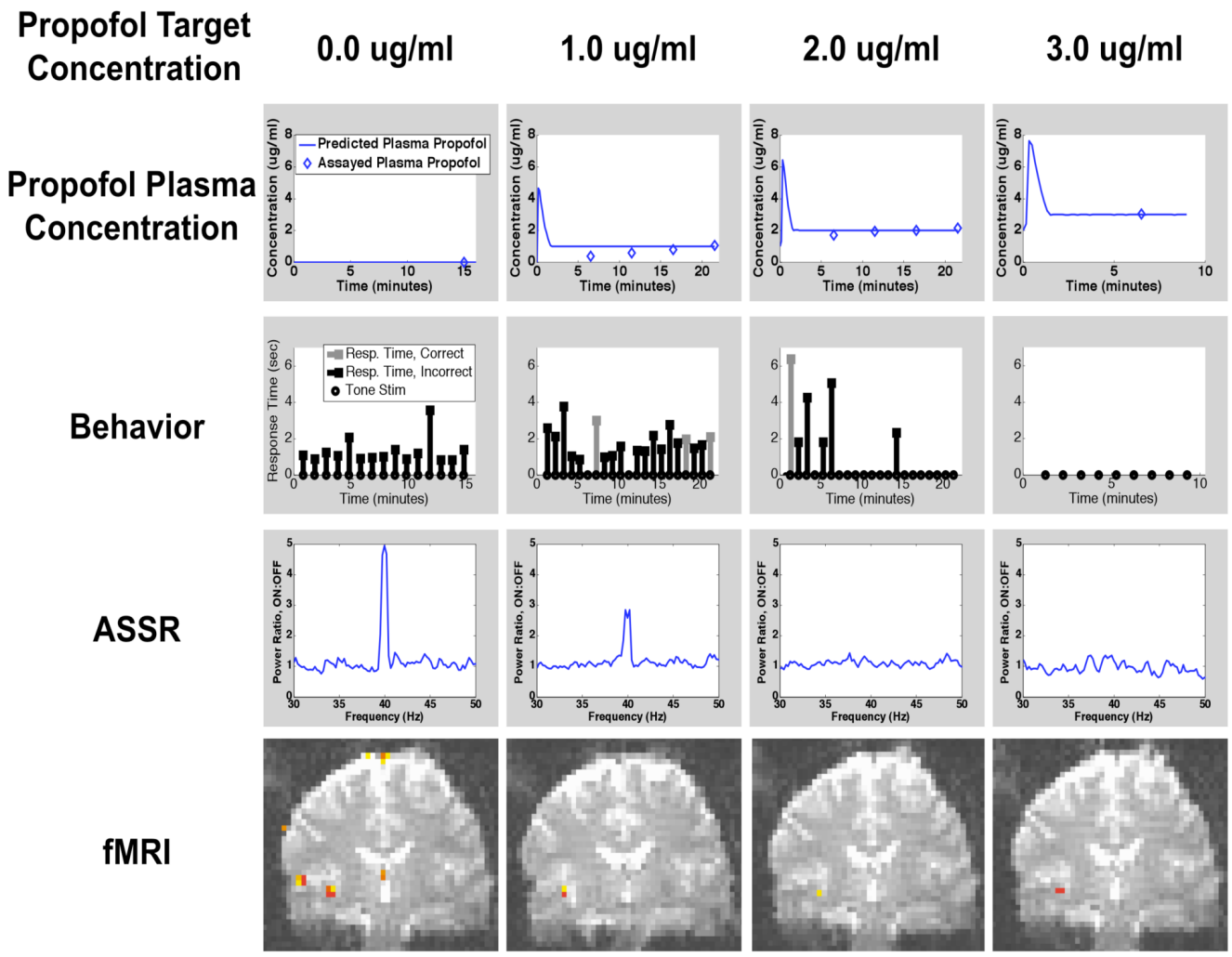

Figure 4.
Time course of predicted and measured plasma propofol concentrations, behavioral responses, ASSR, and fMRI during increasing doses of propofol in a representative study subject.

Table 1

Measured PCO_2 levels and deviation of PCO_2 from baseline by level and subject. Deviation of PCO_2 from baseline was analyzed with a one-way ANOVA using Scheffe's method for multiple comparisons, showing no significant change in PCO_2 levels from baseline.

Measured PCO_2 Levels									
Level	**Subject 1**	**Subject 2**	**Subject 3**	**Subject 4**	**Subject 5**	**Subject 6**	**Subject 7**	**Average**	**Std. Dev.**
Baseline	44	**	43.1	32.9	32.8	34.8	38.1	37.2	4.5
Level 1	41.1	44.6	45.4	34.7	26	30.3	39.6	37.4	7.3
Level 2	40.3	43	47.4	39.2	30.1	35.9	33.6	38.5	5.8
Level 3	45	45.1	44.5	41.8	28.4	38.5	33.4	39.5	6.5
Level 4	*	48.3	***	33.9	27.7	37	36.4	36.7	7.5
Deviation of PCO_2 from Baseline									
Level	**Subject 1**	**Subject 2**	**Subject 3**	**Subject 4**	**Subject 5**	**Subject 6**	**Subject 7**	**Average**	**Std. Dev.**
Baseline	0	**	0	0	0	0	0	0.0	0.00
Level 1	−2.9		2.3	1.8	−6.8	−4.5	1.5	−1.4	1.77
Level 2	−3.7		4.3	6.3	−2.7	1.1	−4.5	0.1	1.77
Level 3	1		1.4	8.9	−4.4	3.7	−4.7	1.0	1.77
Level 4	*		***	1	−5.1	2.2	−1.7	−0.9	2.16

* = Subject 1 did not reach level 4;

** = Baseline PCO_2 measurements were not available for Subject 2

*** = Level 4 PCO_2 measurements were not available for Subject 2.)